Precursory Patterns, Evolution and Physical Interpretation of the 2025 Santorini-Amorgos Seismic Sequence

Davide Zaccagnino[a,b], Georgios Michas[c], Luciano Telesca[d], Filippos Vallianatos[e,f]

[a]*Institute of Risk Analysis, Prediction and Management (Risks-X), Southern University of Science and Technology (SUSTech), 1088 Xueyuan Rd., Nanshan, Shenzhen, 518055, Guangdong, China*
[b]*National Institute of Geophysics and Volcanology (INGV), Via di Vigna Murata, 605, Roma, 00143, Italy*
[c]*Institute of Geodynamics, National Observatory of Athens, Lofos Nymfon, Athens, 11810, Greece*
[d]*Institute of Methodologies for Environmental Analysis, National Research Council, Zona Industriale C.P. 27, Tito Scalo, 85050, Italy*
[e]*Section of Geophysics-Geothermics, Department of Geology and Geoenvironment, National and Kapodistrian University of Athens, Panepistimiopolis - Zographou, Athens, 15784, Greece*
[f]*Institute of Physics of Earth's Interior and Geohazards, UNESCO Chair on Solid Earth Physics and Geohazards Risk Reduction, Hellenic Mediterranean University Research and Innovation Center, Romanou 3 Chalepa, Chania, 73133, Greece*

Abstract

The 2025 Santorini-Amorgos seismic sequence marked a significant episode of volcanic-seismic unrest in the Hellenic Volcanic Arc, offering a unique opportunity to investigate precursory patterns and the dynamic evolution of seismicity in a complex tectonic setting. Here, we analyze the preparatory phase of the crisis using a high-resolution relocated seismic catalog, anomaly detection, and statistical modelling. We identify four distinct stages of seismic activity: 1) An initial volcano-driven phase starting in the summer 2024 with slightly accelerating moment release and focusing towards the Amorgos region; it was followed by 2) a progressive onset of the seismic sequence during January associated with stronger clustering, steady b-value and rocketing magnitude entropy with right-shifting multifractal spectrum. 3) A successive very energetic transitional, five-days-long chaotic phase in early February, with evident breakdown of the Gutenberg-Richter law, apparent decrease of the b-value, multifractality and hypocenters super-diffusion. Finally, 4) a terminal sub-diffusive aftershocks-dominated phase occurring after mid-February. Clustering, fractal and entropy analyses reveal significant premonitory changes marked by progressive migration of seismicity towards the area that hosted the sequence. Our findings suggest that the 2025 sequence was promoted by multiscale crustal weakening processes likely triggered by a magmatic-tectonic interaction and governed by the strong segmentation of the Santorini-Amorgos normal-faulting system preventing the strike of a M_w 6+ mainshock.

Keywords: Santorini-Amorgos seismic crisis, Statistical precursory patterns, Earthquake clustering, Fractal analysis, Volcano-triggered tectonic seismicity, Gutenberg-Richter violation

---

Introduction

1. An unprecedented seismic sequence in a volcano-tectonic setting

The Aegean Sea is among the most active geodynamic regions in the Mediterranean area. The Santorini-Amorgos tectonic zone is well-known for its persistent magmato-tectonic activity within the Hellenic Volcanic Arc. This setting is characterized by frequent volcano-tectonic processes, with several submarine volcanic cones aligning in a SW-NE direction, parallel to the regional tectonic features (Nomikou et al., 2012; Hooft et al., 2017). The most prominent is the submarine Kolumbo volcano, which last erupted in 1650 CE and hosts widespread microseismicity (Schmid et al., 2022). Since the summer 2024, seismic activity started to raise in the area of the Santorini region, driven by the progressive uplift of the caldera (Lippiello et al., 2025). At the end of January 2025, an unprecedented seismic sequence, in terms of rates and magnitudes, started to evolve in the offshore region to north-east of the Santorini volcanic complex, in the Santorini-Amorgos tectonic zone (Fig. 1). This seismic sequence evolved as a swarm, lacking a large rupture that could be considered a mainshock, and included numerous events with magnitudes greater than four, reaching up to magnitude 5.3 (NOAIG - Institute of Geodynamics, National Observatory of Athens, 2025). The cumulative energy nucleated at the peak of seismic activity lasted about four days and was roughly equivalent to a M_w 6.2 earthquake Lippiello et al. (2025). The 2025 crisis was preceded by nearly six months of escalating unrest within Santorini's caldera, highlighted by progressive deformation, elevated carbon

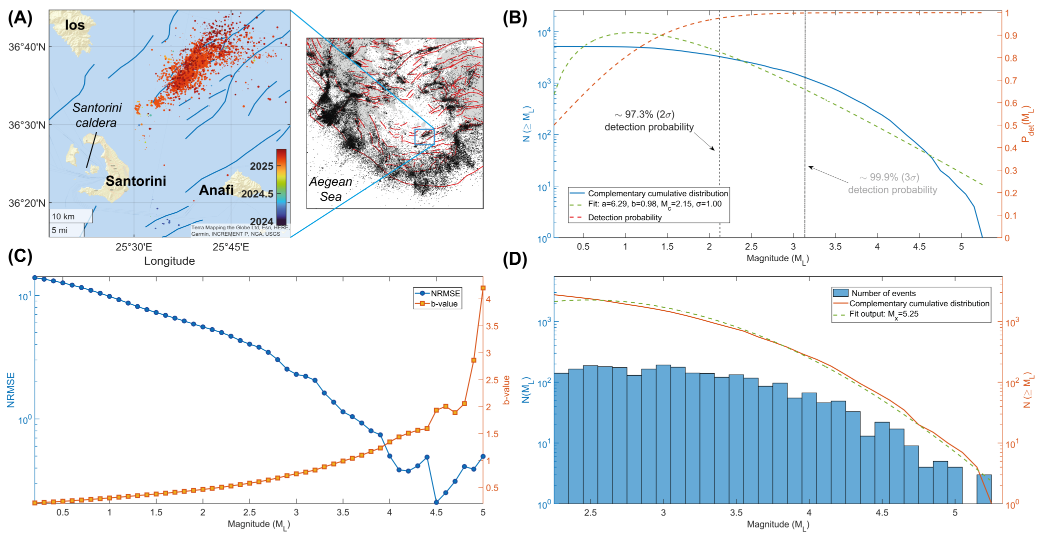

Figure 1: The 2024-2025 seismicity in the Santorini-Amorgos area. (A) A map of the shallow (depth smaller than 30 km) $M_L \geq 2.2$ seismic events occurred from January 1, 2024 to April 30, 2025. Faults are after Leclerc et al. (2024) (B) The Santorini-Amorgos seismic activity shows a clear violation of the expected Gutenberg-Richter law as proven by the instability of the b-value estimation throughout the whole spectrum of magnitudes (orange line) and the corresponding decreasing normalised root mean square error (NRMSE, blue line) (C), so that we combined a Gaussian detection function (its cumulative distribution is represented by the dashed red line in (B)) and a Kagan's gamma function (green dashed line in (B)) to better reproduce the frequency-size distribution of magnitudes. The final joint result of our fit is shown in (D).

dioxide emissions and anomalous microseismicity. These precursory signals mirrored patterns observed during past episodes of volcanic unrest, such as the 2011–2012 Santorini inflation episode (Newman et al., 2012; Vallianatos et al., 2013), but with quantitative differences in spatial extension and energy release. The seismic swarm started in late January 2025 and coincided with a rapid migration of hypocenters from the Kolumbo submarine volcano region towards the Santorini-Amorgos graben system, suggesting a transition from localized fluid-driven fracturing to regional tectonic stress release. Since late February 2025, the seismic rate has been decaying rapidly; at the same time, focal mechanisms shifted from a regime with significant isotropic components (Zahradnik et al., 2025) to regular shear events. This trend suggests a transition from fluid-mediated seismicity triggering to an Omori-like aftershocks dynamics.

Open questions and research direction

The fundamental mechanisms driving the initiation and progression of the Santorini-Amorgos seismic sequence have already been extensively documented in recent studies (NOAIG - Institute of Geodynamics, National Observatory of Athens, 2025; Lippiello et al., 2025; Karavias et al., 2025; Zahradnik et al., 2025), revealing a well-established framework of magmatic-tectonic interactions. However, the exceptional characteristics of this sequence present both a challenge to conventional earthquake rupture models (Kanamori and Brodsky, 2004; Hill et al., 2015) and a unique opportunity to study the complex interplay between magmatic fluids, tectonic stress, and crustal heterogeneity in volcanic arc environments. Unlike typical tectonic earthquakes where reliable precursors remain elusive (Zechar and Zhuang, 2010; Zaccagnino et al., 2024), this sequence exhibits clear precursory patterns and distinctive statistical properties that deviate from standard seismological dynamics. The anomalous features include:

- suppressed maximum magnitudes inconsistent with regional scaling relations (Papazachos and Papazachou, 2003);
- breakdown of the Gutenberg-Richter distribution with reasons beyond the usual catalog incompleteness;
- strongly time-dependent multifractal clustering with breaking during the peak of seismic activity;

- self-sustained swarm-like dynamics.

To systematically investigate these phenomena, we integrate physical modeling of diffusive and entropic processes with advanced statistical analyses including clustering analysis, frequency-size scaling with tapered distributions (Kagan, 2002) also investigating the effect of earthquake detection (Ogata, 1988), multifractal detrended fluctuation analysis (MFDFA) (Kantelhardt et al., 2002) and others. This integrated approach enables the identification of distinct seismic phases within the Santorini-Amorgos sequence and provides quantitative characterization of its anomalous properties yielding new insights into the underlying physical processes governing seismicity in complex volcano-tectonic regions.

Methods and Analysis

Data selection and pre-processing

The Santorini-Amorgos seismicity is found to follow a quite complex frequency-size distribution of magnitudes (Fig. 1B, D). We confirm this result after homogenization of magnitudes (from M_L and other estimates to M_w following empirical calibrations (Papazachos and Papazachou, 2003; Karakostas et al., 2015)) The Gutenberg-Richter law explains very poorly the observed scaling of magnitudes for two reasons: smaller magnitudes are not detected appropriately up to quite high large sizes due to a combination of short-term incompleteness and remote, sea localization of seismicity; moreover, an anomalous number of events with magnitude above 4.5 is reported in the catalog we analyse (NOAIG, 2025) with respect to the maximum registered magnitude. Therefore, we combine three different effects within the same distribution to reproduce the observed scaling of magnitudes, M:

- The Gutenberg-Richter law (Gutenberg and Richter, 1944): $N(M) = 10^{a-bM}$;

- Ogata's Gaussian detection threshold (Ogata, 1993):

$$f_{det}(M) = \frac{1}{2}\left[1 + \text{erf}\left(\frac{M - M_c}{\sqrt{2}\sigma}\right)\right], \tag{1}$$

  where M_c is the so-called completeness magnitude and σ controls the width of the detection threshold.

- Kagan's corner magnitude M_x (Kagan, 2002) with exponential taper:

$$T(M) = \exp\left[-\frac{10^{b(M_x-M)}-1}{b\ln 10}\right] \tag{2}$$

Then, we fit the following generalized distribution

$$G(M) = N(M) \times f_{det}(M) \times T(M). \tag{3}$$

Henceforth, we only consider events with magnitudes with at least 97.3% probability to be detected ($M_c \rightarrow M_c + 2\sigma$) in order to avoid biases in the estimation of important parameters due to short-term aftershock incompleteness ($M_c \simeq 2.2$). The b-value of the Gutenberg-Richter law over time is estimated using the b-positive method (Van der Elst, 2021) with a threshold magnitude equal to 0.4 instead of 0.2 in order to get more stable results. The time-dependent analysis is performed using a moving window with 300 events for the b-value and 200 events for other geophysical quantities of interest except for the fractal dimension, which is calculated using 500 events.

Clustering and Entropy analysis

The Shannon entropy (H) provides a measure of the fluctuations and variability of earthquake magnitudes, m_i, with probabilities (i.e., the frequency of observation in each time window) $p(x_i)$. It is given by (Shannon, 1948)

$$H = -\sum_{i=1}^{N} p(x_i)\log p(x_i), \tag{4}$$

where N is the number of events in each window. Analogously, the Tsallis Entropy, S_{q} generalizes the Shannon entropy with parameter q (Tsallis, 1988) providing insights to properties such as magnitudes, regardless of the scale Telesca et al. (2004); Vallianatos et al. (2016):

$$S_q = \frac{1}{q-1}\left(1 - \sum_{i=1}^{N} p(x_i)^q\right). \tag{5}$$

For $q \rightarrow 1$, S_q converges to H. Higher values of the entropy, both H and S, suggest a more chaotic and unpredictable behavior of the system.

Spatial-temporal analysis

In our analysis we study the trends of the interevent times, Δt_i, and space, $\|\mathbf{x}_{i+1}-\mathbf{x}_i\|$, defined as the time and distance in between two successive events above the minimum selected magnitude. Moreover, we characterize the diffusive properties of seismicity in space and time using both classical diffusion, i.e., assuming, as a first hypothesis, that the mean squared displacement grows linearly with time $\langle r^2(t)\rangle = 2dDt$, where d is dimension ($d = 2$ for epicenters and $d = 3$ for hypocenters) and D is the diffusion coefficient (Metzler and Klafter, 2000).
For N events in the time window with locations $\mathbf{x}_i$, the diffusion coefficient is given by

$$D = \frac{1}{2d(N-1)} \sum_{i=1}^{N-1} \frac{\|\mathbf{x}_{i+1} - \mathbf{x}_i\|^2}{\Delta t_i}. \tag{6}$$

Anyway, it is often the case that the hypothesis above is not a good approximation of reality; therefore, we generalize our analysis to the so-called "anomalous diffusion", where the mean squared displacement follows $\langle r^2(t)\rangle \propto t^\alpha$ (Michas and Vallianatos, 2018). If $\alpha < 1$, a sub-diffusive process occurs controlled by disorder within complex settings such as stress trapping within fractured fault systems with very slow spatial spreading, while super-diffusion is obtained for $\alpha > 1$ with rapid stress transfer. If $\alpha = 1$ we recover the classical case. For anomalous cases, the estimate of α is performed via log-log slope calculation of the mean squared displacement vs time.

Assessment of clustering

The global coefficient of variation, C_V, is calculated to quantify the temporal clustering of seismicity by comparing interevent time variability to a Poisson process (Cox and Lewis, 1966):

$$C_V = \frac{\sigma_{\Delta t}}{\langle \Delta t\rangle} \tag{7}$$

where $\sigma_{\Delta t}$ and $< \Delta t >$ are the standard deviation and mean of interevent times. $C_V > 1$ indicates clustering, while $C_V \approx 1$ suggests Poissonian behavior; values below one stand for regular recurrences.

Criticality

For a more refined measure of how seismicity evolves over time, the branching ratio, n, measures criticality (i.e., tendency to develop long-range interactions following power-laws with universal exponents and sensitivity to perturbations) and it is defined as the ratio between triggered and total number of seismic events (Ogata, 1988). We estimated it via maximum likelihood in a space-variable background intensity ETAS model (Nandan and Sornette, 2022). A branching ratio $n \approx 1$ marks criticality, $n > 1$ supercriticality, and $n < 1$ subcriticality (Helmstetter and Sornette, 2003).

Fractal analysis

Fractal correlation dimension

A first rough glimpse onto the fractal properties of seismicity can be provided by the correlation dimension, D_2, which can be used to characterize the spatial clustering of hypocenters (Grassberger and Procaccia, 1983). For N events (we use a moving window with 500 events), the correlation sum (integral), $C(r)$, counts the pairs of hypocenters within a distance r:

$$C(r) = \frac{2}{N(N-1)} \sum_{i<j} \Theta(r - \|\mathbf{x}_i - \mathbf{x}_j\|), \tag{8}$$

where Θ stands for the Heaviside step function. D_2 is estimated as the slope of the line from the scaling region of $\log C(r)$ vs. $\log r$. Anyway, the suitable selection of the region where the log-log plot follows a linear trend is not easy. To improve robustness, we fit $C(r)$ with a sigmoid function:

$$C(r) = y_0 + \frac{k}{1 + e^{-\gamma(r-r_0)}}, \tag{9}$$

where k essentially controls the slope. Then, the fractal dimension D_2 (Kagan, 2007) is the slope of the sigmoid function in its inflection point, i.e., the derivative at the saddle point $r = r_0$:

$$D_2 = \left. \frac{d \log C(r)}{d \log r} \right|_{r=r_0} = \frac{k\gamma}{4}. \tag{10}$$

Multifractal analysis

The analysis of the multifractal spectrum, $f(\alpha)$, is an advanced technique to characterize the scaling properties of earthquake magnitudes and interevent times (Telesca and Lapenna, 2006). Specifically, the Multifractal Detrended Fluctuation Analysis (MFDFA) evaluates the scaling properties in non-stationary earthquake time series (we apply it to earthquake magnitudes and interevent times). It is implemented following the seminal work by Kantelhardt and colleagues (Kantelhardt et al., 2002). For a time series x_i of length N, where x can represent both magnitudes or interevent times, the integrated profile of residuals with respect to the mean value, $\langle x\rangle$, $Y(i) = \sum_{k=1}^{i}[x_k - \langle x\rangle]$ is computed. The profile is segmented into $N_s = \lfloor N/s \rfloor$ non-overlapping intervals of scale s, with a reverse segmentation to include residual data. For each segment, a polynomial $P^{(r)}$ of order r is fitted to remove local trends, and the variance $F^2(s)$ is calculated around this trend. The choice of r depends on the data: linear detrending ($r = 1$) is usually sufficient for weakly non-stationary trends, while higher orders ($r \geq 2$) are needed for stronger nonlinearity. Then, the q-th order fluctuation function $F_q(s)$ is derived by averaging variances across segments. If $F_q(s) \sim s^{H(q)}$ with $H(q)$ decreasing as q increases, the dynamics is multifractal and featured by the so-called generalized Hurst exponent $H(q)$. Then, a quantitative and visual technique to investigate the scaling properties of interevent times and magnitudes consists in plotting their multifractal spectrum $f(\alpha)$ defined as (Kantelhardt et al., 2002)

$$f(\alpha) = q[\alpha - h(q)] + 1, \tag{11}$$

where $\alpha = h(q) + q\frac{dh(q)}{dq}$.
We followed the steps discussed in (Ihlen, 2012) to set up our code. We profile the multifractal spectrum over the temporal evolution of seismicity by separating events above the minimum considered magnitude into four different phases highlighted by using the techniques described above. The shape of $f(\alpha)$ is incredibly rich in information about the statistical properties of seismicity:

- A wide spectrum indicates strong multifractality, i.e., a single dimension is poorly informative about the complex time and magnitude dynamics of the events;
- Left-skewed (right-skewed) spectra suggest dominance of large (small) fluctuations of magnitudes/inter-events (Shimizu et al., 2002);
- The α range provides a measure of heterogeneity in scaling; more, specifically, higher values of α suggest strong heterogeneity.

Results

Our analysis of the Santorini-Amorgos seismicity ($M \geq 2.2$) from January 2024 to April 2025 reveals four distinct phases of seismic activation. A first sign of activity is detected in summer 2024 with a preparatory phase characterized by decreasing interevent distances (Figure 2) and coherent fluctuations in interevent times (Figure 3). During this initial stage, we observed a strong positive correlation (up to $r \sim 0.62$) between these parameters, indicating coupled spatial-temporal clustering. This correlation abruptly vanished immediately prior to the major seismic activation in late January 2025. The branching ratio analysis (Figure 4) showed sub-critical behavior throughout 2024 ($n \approx 0.38 \pm 0.02$), suggesting stable stress accumulation. The onset of major seismicity triggered a rapid transition to supercritical dynamics ($n \approx 1.1$), followed by intermittent subcritical-supercritical oscillations before settling into sustained subcritical decay ($n < 0.5 - 0.6$) by April 2025. Concurrently, the b-value (calculated via the b-positive method) decreased progressively from 1.2 ± 0.2 to 0.6 ± 0.05 (Figure 5) in a few weeks in January 2025, consistent with stress localization. Diffusion analysis revealed three distinct transport regimes: initial fast diffusion ($D \simeq 10$ km^2/day, see Figure 6) associated with a super-diffusive behavior ($\alpha > 1$), and terminal long-term sub-diffusion ($\alpha = 0.03$–0.05). The estimation of the diffusion coefficient over time using classical diffusion process, although with large fluctuations, appears stable (Figure 6B) suggesting that anomalous diffusion processes may play a major role and classical diffusion performs poorly for modeling the much more complicated dynamics and space-time evolution of seismicity during the Santorini-Amorgos seismic crisis. No significant depth- or magnitude-dependent trends were observed. Entropy metrics, i.e., both the Shannon and Tsallis entropy, (Figure 7) exhibit a gradual pre-seismic decline, an activation-phase peak, and subsequent decay. The fractal correlation dimension (Figure 8) showed progressive increase until early February 2025, followed by abrupt collapse ($\Delta D_2 \approx 0.3$ over a few days) and linear decay over time. The multifractal analysis (Figure 9) is performed considering the four phases highlighted by previous investigations: we get a broad left-skewed spectrum (until January 2025), a narrowed right-shifted spectrum (since January 26, 2025); we also observe multifractality breakdown (February 2-9), and, at last, partial recovery.

Discussions

Four Phases of Seismicity and Their Physical Interpretation

Our analysis reveals four different phases characterizing the Santorini-Amorgos regional seismicity during January 2024 to April 2025, each with

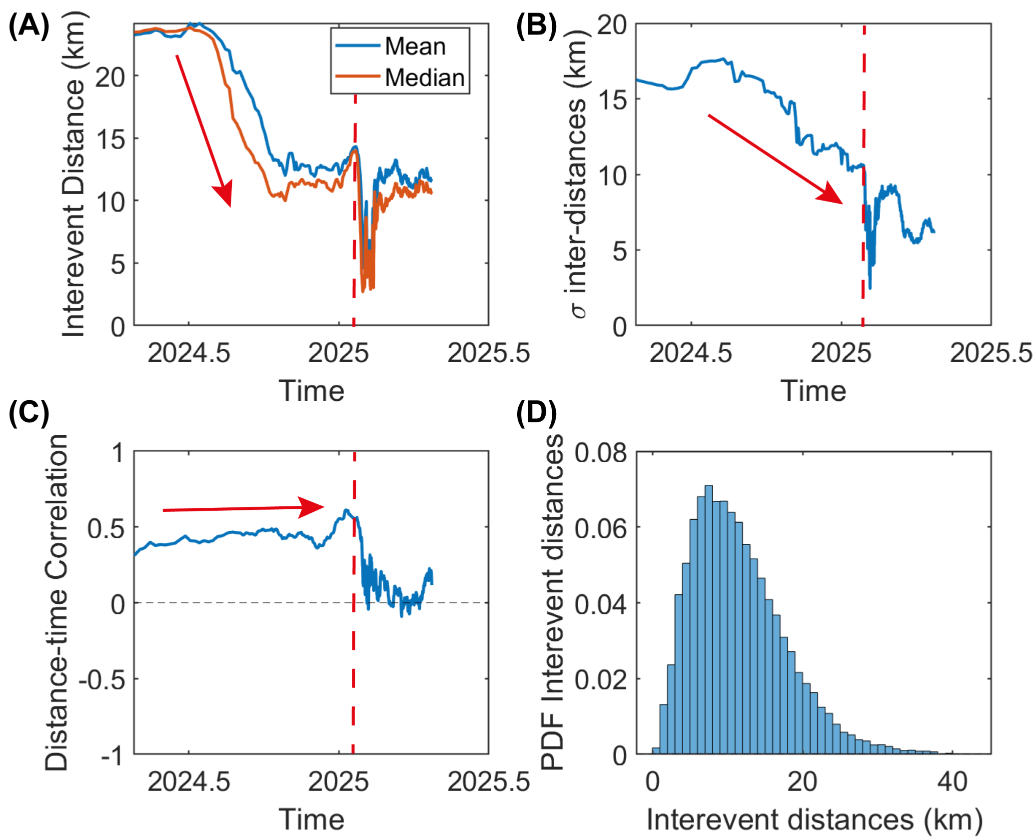

Figure 2: Temporal investigation of (A) the interevent distances between successive seismic events above $M_L 2.2$, (B) standard deviation of such distances and (C) Pearson's correlation coefficient between interevent times and distances. These observations suggest a progressive focusing process of seismicity towards the Amorgos region starting during the summer 2024 promoted by the inflation of the Santorini caldera. (D) Distribution of inter-distances of successive seismic events in the Santorini-Amorgos region.

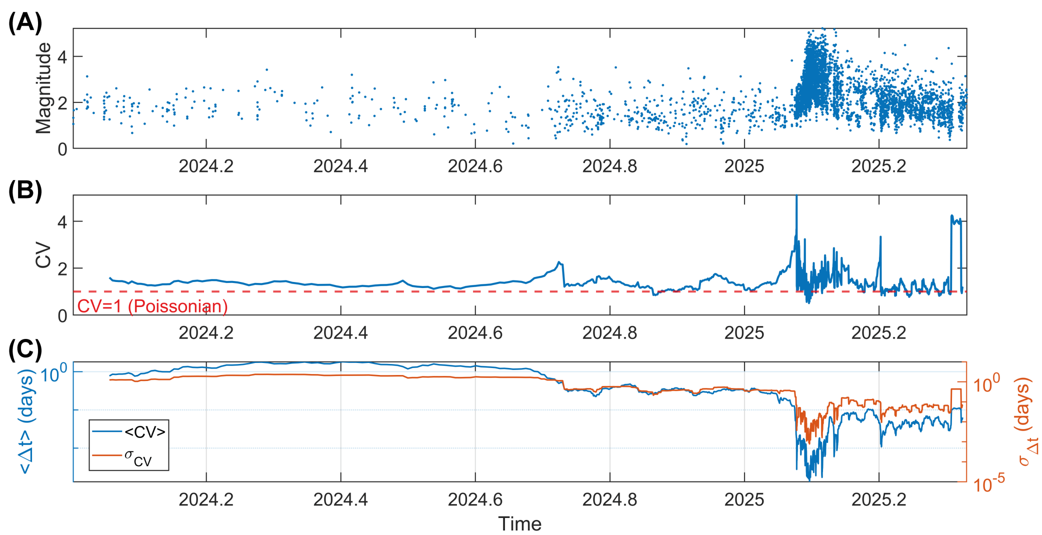

Figure 3: Temporal clustering of seismicity in the Santorini-Amorgos region from January 2024 to April 2025. The global coefficient of variation shows that seismic activity tends to be slightly clustered with a few weeks-long increasing trend observed before the onset of the sequence; coherently, the interevent times and their fluctuations progressively decreased. If considered together with results shown in Figure 2, the acceleration of seismic occurrence supports the idea that a process of stress transfer from the Santorini Caldera triggered instability in the nearby tectonic setting.

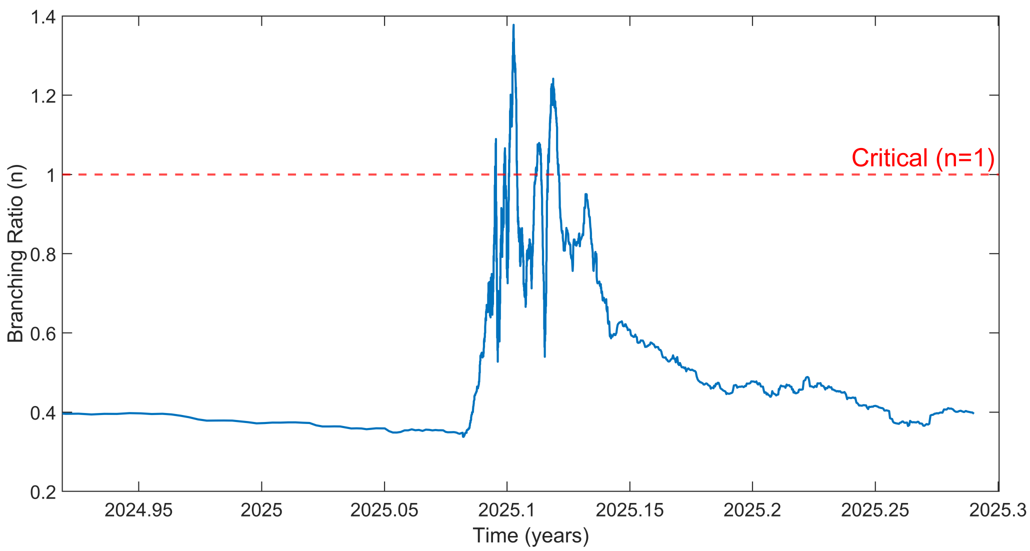

Figure 4: Investigation of criticality in seismicity during the 2025 Santorini-Amorgos seismic sequence. Only shallow seismic events above the selected minimum considered magnitude are used for the computation of the branching ratio. The plot shows that seismicity laid below criticality, most of the time, except for an intermittent phase lasted about two weeks where a recurrent reinforcement of seismic activity promoted the occurrence of several events with magnitudes larger than 4.0.

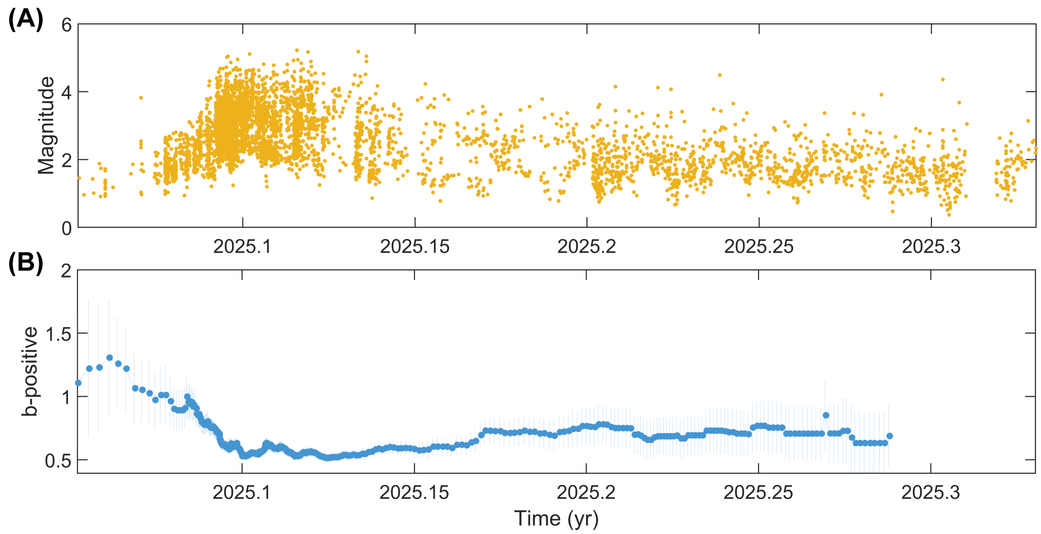

Figure 5: Scaling properties of seismic activity during the Santorini-Amorgos seismic sequence in 2025. The b-value estimated using the b-positive algorithm does not show a clear trend at the onset of the cluster being the uncertainty quite large; then, a progressive decrease is observed up to anomalously low values ($\sim$ 0.6-0.7).

unique spatial-temporal, statistical and dynamical features unveiled by the integration of different techniques we implemented.

Preparatory Phase (Summer 2024 - January 25, 2025)

The initial stage is characterized by decreasing interevent distances (Fig. 2) and coherent fluctuations in interevent times (Fig. 3); the two quantities resulted to be quite well spatial-temporal correlated with a long-term positive trend culminating just before the onset of major seismicity ($\rho \sim 0.62$). This suggests coupled clustering, likely reflecting progressive stress accumulation in a localized volume at the edge of instability, in agreement with established models (Dieterich, 1994). The subcritical branching ratio ($n \approx 0.38 \pm 0.02$) indicates stable background seismicity without significant triggering (Helmstetter and Sornette, 2003). Our interpretation is in agreement with upcoming research results (Lippiello et al., 2025), i.e., volcano-magmatic driven stress transfer to north-east likely mediated by fluid migration.

Critical Transition (Late January 2025)

The abrupt loss of spatial-temporal correlation accompanied the major activation, consistent with a critical system approaching instability (Sornette,

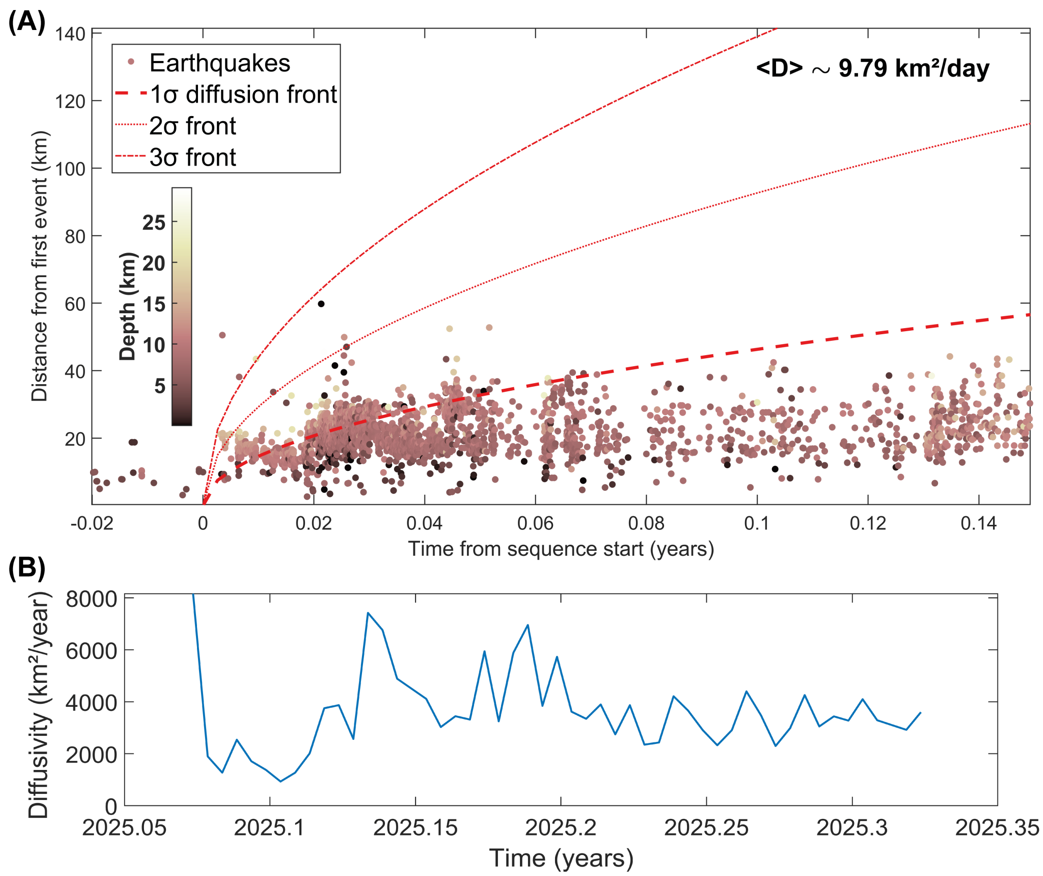

Figure 6: Diffusive behavior of seismic activity during the Santorini-Amorgos seismic sequence in 2025. Classical diffusion captures the spatial spreading of seismicity during the early stage, with a diffusion coefficient $D \sim 10\ km^2/day$. A short second phase is also observed (read the main text) featured by a strongly super-diffusive dynamics followed by a clearly sub-diffusive trend lasting for a few months.

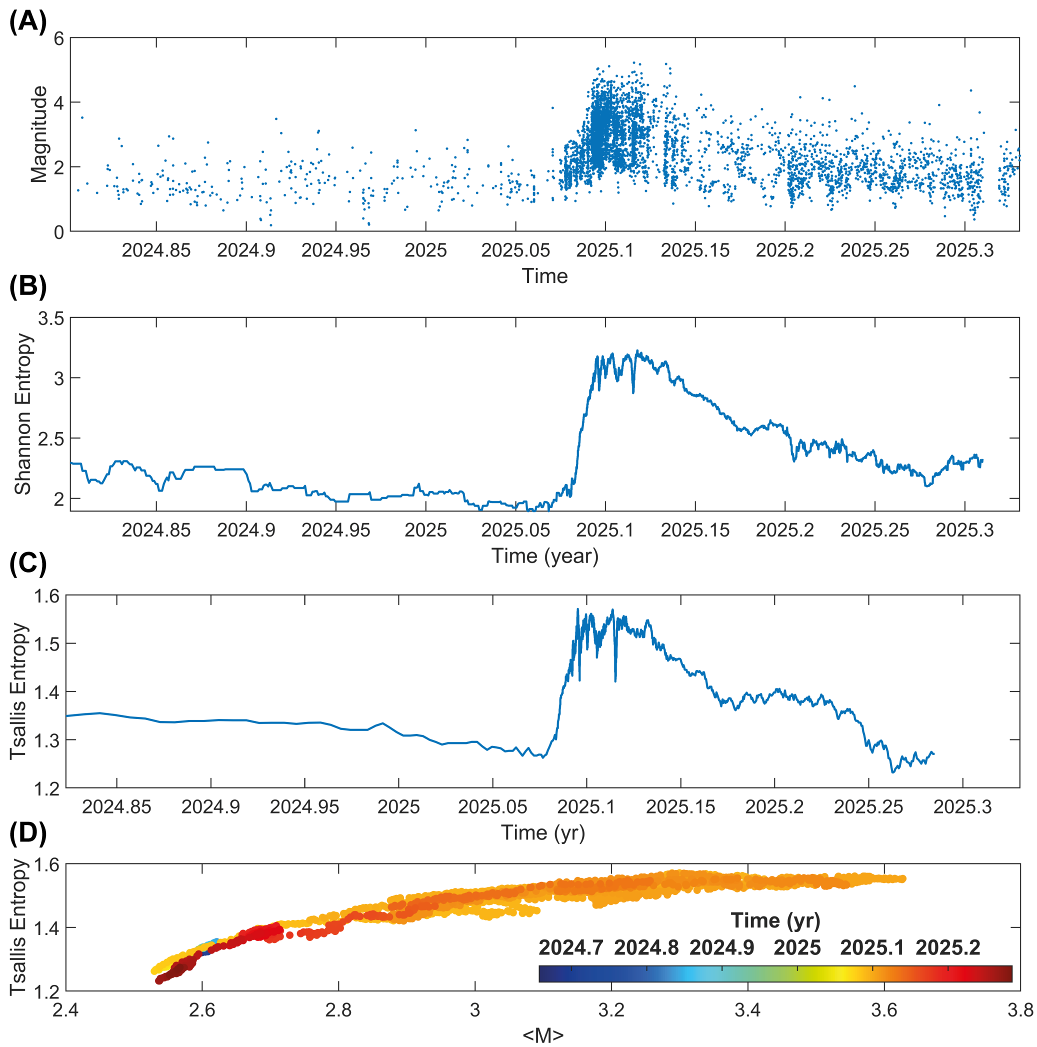

Figure 7: Analysis of the Shannon and Tsallis entropy of magnitudes over time during the Santorini-Amorgos 2024-2025 seismicity. A slightly decreasing trend is observed until the onset of the major cluster in the late January 2025, when a swift increase is observed.

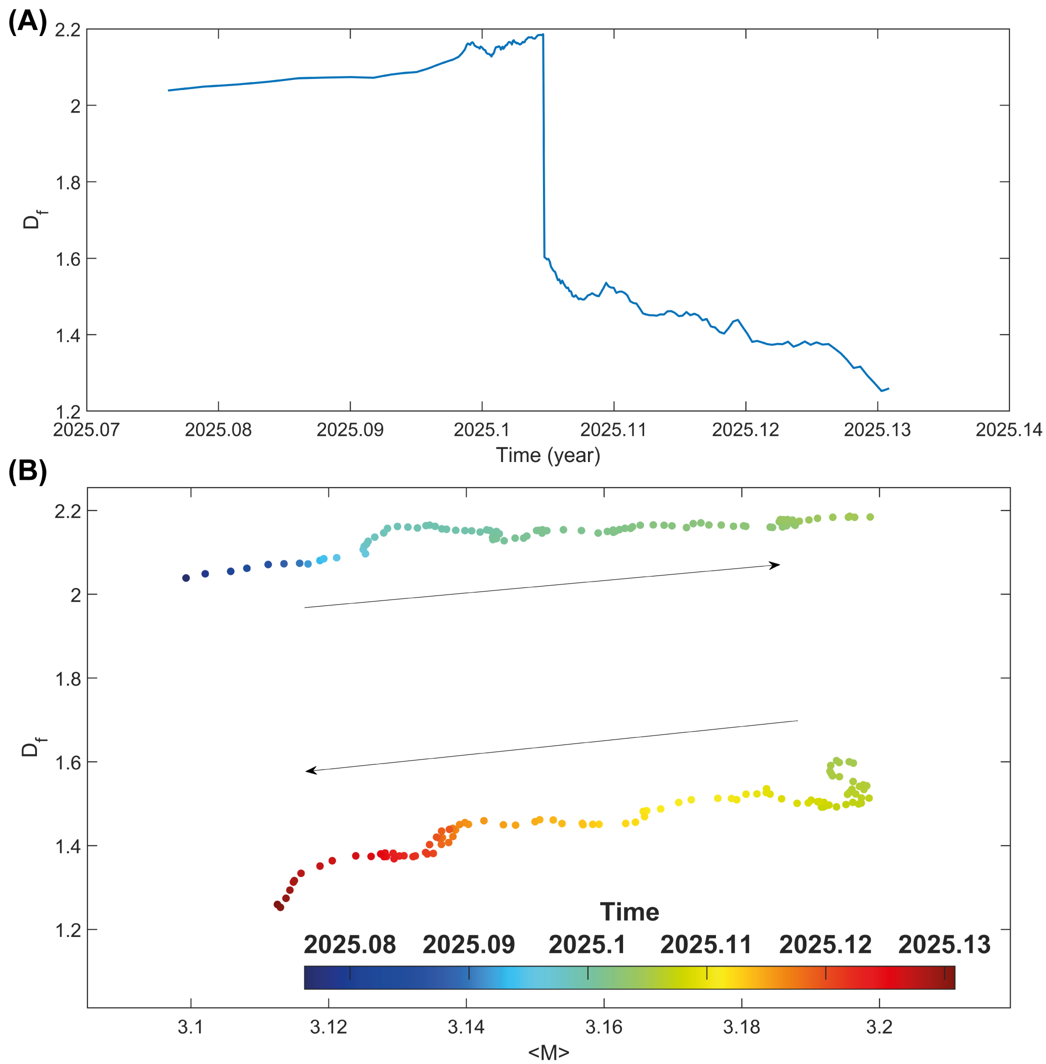

Figure 8: Assessment of the fractal correlation dimension of hypocenters during the Santorini-Amorgos 2025 seismicity using a 500 events moving window with one-quake steps. The fractal dimension increases progressively in the first phase; then, the contribution of an extremely productive phase starting on February 2-3, 2025, produces an apparent drop of the fractal dimension, likely affected by higher magnitude incompleteness of the catalog. Anyway, the successive long-lasting trend confirms a progressive decrease of the fractal dimension coherent with the observed lowering of the b-value of seismicity.

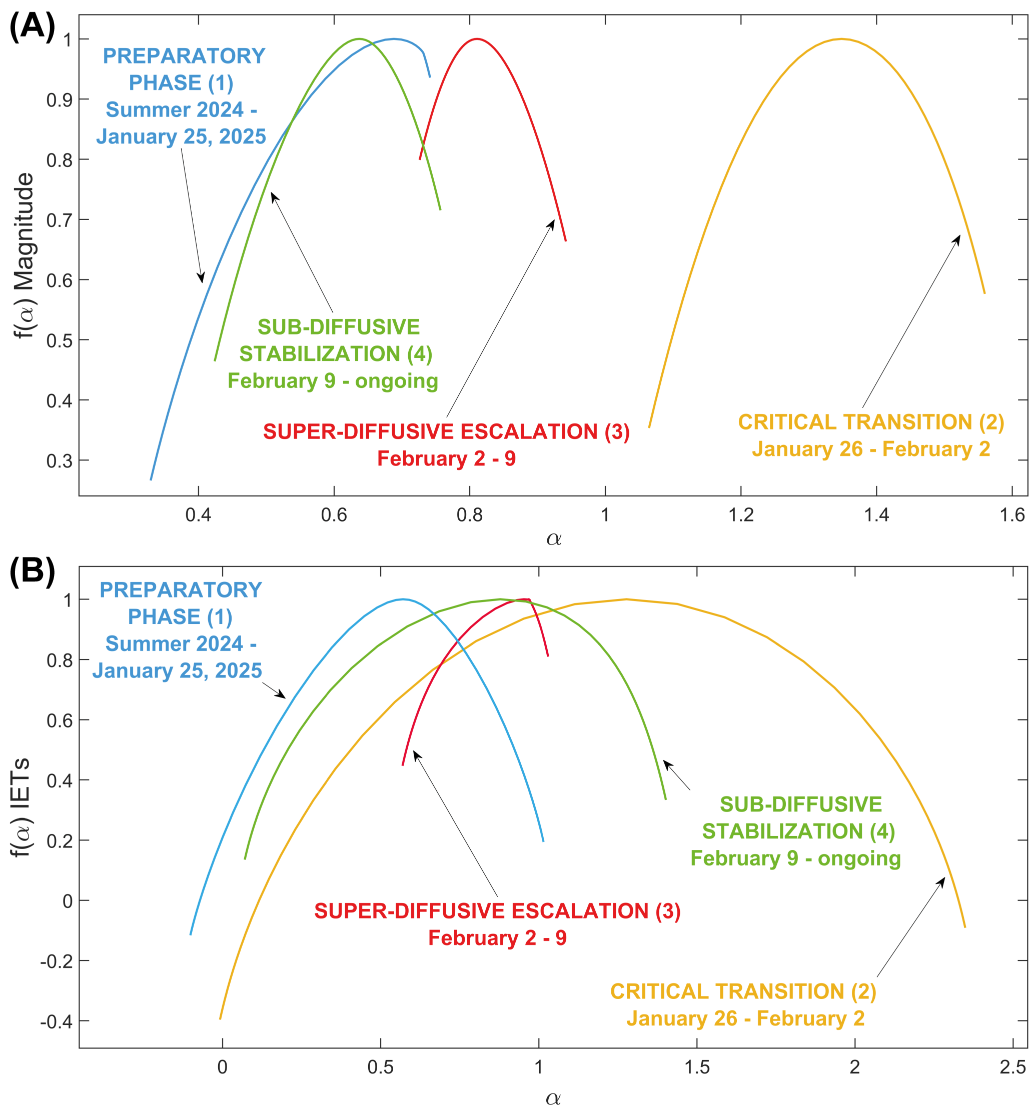

Figure 9: Multifractal spectra realized by means of linear interpolating polynomials of magnitudes (A) and interevent times (B) over the four different phases of the seismic activity in the Santorini-Amorgos region.

2006). It is consistent with the observed rapid transition to (super)critical dynamics ($n \approx 1.1$) and b-value progressive drop (from 1.2 ± 0.2 to ~ 0.60) suggesting stress localization and increased fault coupling (Schorlemmer and Wiemer, 2005). This phase marks the transition from a volcano-magmatic-mediated seismicity to an avalanche-like dynamics in a strongly segmented and structurally complex normal-faulting system.

Super-diffusive Escalation (February 2-9, 2025)

We observe a fast diffusion regime (even though poorly constrained by a $D \simeq 10$ km^2/day, with $\alpha > 1$), which implies fluid-driven stress transfer mixed with cascading failure (Shapiro et al., 2005; Michas, 2025). The subsequent breakdown of multifractality (Fig. 9) may reflect a tendency to a larger homogeneity of the time/magnitude dynamics of the seismic process, as already detected in previous seismic sequences (Telesca and Lapenna, 2006).

Sub-diffusive Stabilization (Mid February–April 2025)

The last stage is characterized by sub-diffusion ($\alpha = 0.03$–0.05 km^2/day) and fractal dimension progressive lowering ($\Delta D_2 \approx 1.3$) correlated with a slight decay of the b-value indicating stress homogenization and transition to seismic quiescence typical of aftershocks relaxation dynamics (Ben-Zion and Sammis, 2003).

2. Abnormal moderate size events and no mainshock

One of the most stunning features of the Santorini-Amorgos seismic sequence is the statistical dominance of moderate events ($4 \leq M \leq 5.3$) without a large mainshock, to be added to the breaking of the usual Gutenberg-Richter scaling. Hereafter, we discuss the possible origins of such an anomaly.

- The few-days sustained intermittently supercritical branching ratio ($n \approx 1.1$) and the concomitant anomalous diffusion suggest widespread instability associated with energy dissipation through swarm-like activity rather than a single repeatedly-activated large rupture (Fischer et al., 2023). Even the spatial-temporal distribution of epicenters show that several different seismogenetic structures have been involved.

- Complementary to the previous explanation, the fractal dimension increase followed by sudden drops (Fig. 8) hints at a strongly segmented fault system inhibiting rupture coalescence (Kagan, 1991). This viewpoint is also supported by the measure of quite high b-value during the second phase of seismicity ($b = 1.0 - 1.4$), as discussed in previous research works (Zaccagnino et al., 2023).

- Moreover, a role of volcano-magmatic-tectonic interaction is highlighted by the progressive b-value decline to ~ 0.6. It may also imply, together with fault segmentation, high differential stress within the normal fault system, so that the absence of a major event might reflect aseismic slip fostered by high temperature gradients and sudden percolation of highly-pressurized fluids into preexisting fracture networks, with subsequent seismic activity mediated by fluid pressure gradient smoothing and stress transfer from previous earthquakes. This scenario has already been proposed in other volcano-tectonic environments (e.g., at Mount Rainer (Shelly et al., 2013) and Yellowstone (Farrell et al., 2009)).

3. Comparative dynamics and key Lessons from the 2025 Santorini-Amorgos seismic sequence

The 2025 Santorini seismic sequence exhibits hybrid characteristics that bridge tectonic and volcanic swarms. Like tectonic seismicity (Nishikawa and Ide, 2017; Passarelli et al., 2018), it displays a low corner magnitude with no dominant mainshock, sustained activity violating the Omori's law, and alternating super-diffusive ($\alpha > 1$) and classical diffusive ($\alpha \approx 1$) epicenter migration. Simultaneously, it shares traits with volcanic swarms (Roman and Cashman, 2006), including positive isotropic components in moment tensors (Zahradnik et al., 2025) and clear geodetic deformation trends (Lippiello et al., 2025). This duality raises fundamental questions about the interplay between magmatic and tectonic forcing, i.e., whether they acted jointly throughout the sequence or if the volcano-magmatic contribution is merely limited to fueling instability into the already stressed normal fault system. This topic is widely debated in literature, but mostly regarding how seismicity triggers eruptions and minor volcanic activity and not vice-versa (Bergman and Solomon, 1990; Uchide et al., 2016; Nishimura, 2017; Sawi and Manga, 2018; Seropian et al., 2021).
Moreover, the sequence provides critical insights into earthquake physics and hazard assessment:

- On the separate and different contributions of deterministic and stochastic dynamics: while the Santorini caldera experienced uplift (excluded from our analysis since we do not included events in the Santorini caldera in our investigation), seismicity in the Amorgos sector showed pronounced changes in clustering metrics, interevent spatial-temporal structure, Shannon and Tsallis entropy, and fractal dimension. Multifractal Detrended Fluctuation Analysis (MFDFA) shows left-drifting spectra for both interevent times and magnitudes during the third and fourth phase (Figures 9), suggesting a deterministic driver with a minor role of stochastic dynamics. This supports the idea that when deterministic processes (e.g., stress transfer, fluid diffusion) play a major role - as often occurs in volcanic settings - seismicity may become more predictable through physics-based monitoring (Ide and Sornette, 2002; Sornette and Helmstetter, 2002). Precursors gain meaningful predictive power when tied to underlying physical mechanisms, emphasizing the need to uncover hidden drivers of seismicity in seemingly stable systems.

- On fault segmentation effects: the prevalence of moderate events without a large mainshock highlights how fault network geometry modulates seismic energy release. High b-values (1.2 ± 0.2 early in the sequence) and elevated fractal dimensions (Fig. 8) point to a highly segmented fault system that inhibited rupture coalescence (Kagan, 1991; Venegas-Aravena and Zaccagnino, 2025). Such segmentation may also explain the fast diffusion observed during the supercritical phase ($D \simeq 10$ km^2/day).

- On the importance of memory effects: persistent memory effects, evidenced by long-range spatial-temporal clustering and recurrent same-magnitude events, deviate from classical mainshock-aftershock statistics (Lennartz et al., 2008; Taroni et al., 2024). This anomaly underscores how background processes (e.g., fluid migration) can override standard scaling laws. Fractal analysis captures these deviations through multifractality breakdowns (Fig. 9) and entropy peaks, as demonstrated in analogous swarms, e.g., Telesca et al. (2015).

- On the stress sensitivity and remote triggering: the sequence sensitivity to minor stress perturbations, evidenced by rapid transitions between sub-critical ($n \approx 0.38$) and supercritical ($n \approx 1.1$) regimes, is consistent with studies showing swarm destabilization near instability thresholds (Gomberg et al., 1997; Yong-Ge et al., 2003; Zaccagnino et al., 2021, 2022). Caldera deformations may have remotely activated the Santorini-Amorgos fault system via static stress transfer or fluid-pressure diffusion, illustrating cascading interactions between volcanic and tectonic systems already detected in analogous regional investigations (Lemarchand and Grasso, 2007).

These observations collectively challenge traditional seismic hazard paradigms, advocating for integrated monitoring combining geodesy, multifractal analysis, and stress transfer modeling in tectonically active volcanic regions.

Conclusions

The analysis of seismicity in the Santorini-Amorgos region from January 2024 to April 2025 reveals a complex four-stage sequence marked by distinct precursory patterns, critical transitions, and post-onset dynamics. The initial phase, characterized by decreasing interevent distances and consistent progressive drop in interevent times, suggests a progressive stress focusing. The strong positive correlation between these quantities before the major seismic activity in late January 2025, followed by a sharp drop, agrees with theoretical expectations of mounting driven-stress instability prior to major events through strain localization on weak fault segments. The subcritical behavior (branching ratio $\sim$0.4) dominating the early phase further supports the idea of a preparatory stage. The transition to supercritical dynamics at the sequence onset, with intermittent sub- and supercritical fluctuations, reflects the system's instability during peak activity. The decrease in b-values from $\sim$1.0 to 0.6 after the sequence initiation suggests a shift toward higher stress release, a phenomenon well-documented in both volcanic, tectonic and injection-induced seismicity (Michas, 2025). The diffusion analysis reveals a progression from super-diffusive to sub-diffusive behavior, indicating evolving energy dissipation mechanisms, consistent with observations from other seismic swarms where initial rapid stress redistribution transitions to slower, confined deformation. Entropy and fractal dimension analyses further corroborate the system's evolving complexity. The initial rise in correlation dimension before the main seismic phase suggests increasing spatial organization of hypocenters, while its abrupt drop and subsequent decline reflect post-onset relaxation. The multifractal behavior, particularly the spectral shifts and temporary breakdown in early February, highlights the dynamic interplay of stress and fracture processes. The suitability of linear polynomial fits for multifractal analysis contrasts with higher-order models may emphasize the dominance of first-order stress interactions in controlling seismicity during the whole process. The Santorini-Amorgos 2025 sequence exhibits features common to both volcano-magmatic and tectonic seismicity: specifically, it is possible that the inflation and subsequent deflation of the Santorini Caldera could trigger seismicity via stress-transfer to north-east towards a marginally-stable highly-fractured normal-faulting tectonic setting. Its extremely segmented structure may be responsible for the extremely high productivity of moderate magnitude events (relatively low corner magnitude) without any large mainshock. In summary, our findings are consistent with previous literature on seismic swarms, induced and volcano-tectonic sequences (e.g., Lemarchand and Grasso (2007); Farrell et al. (2009); Shelly et al. (2013); Uchide et al. (2016); Iaccarino and Picozzi (2023)) and show that a quantitative assessment over the temporal evolution of seismicity is possible even in anomalous cases like the 2025 Santorini-Amorgos seismic sequence, reinforcing the importance of integrated statistical and multifractal approaches for understanding precursory signals and volcano-magmatic triggering mechanisms in seismically active tectonic regions.

References

Ben-Zion, Y., Sammis, C.G., 2003. Characterization of fault zones. Pure and applied geophysics 160, 677–715.

Bergman, E.A., Solomon, S.C., 1990. Earthquake swarms on the mid-atlantic ridge: Products of magmatism or extensional tectonics? Journal of Geophysical Research: Solid Earth 95, 4943–4965.

Cox, D.R., Lewis, P.A., 1966. The statistical analysis of series of events .

Dieterich, J., 1994. A constitutive law for rate of earthquake production and its application to earthquake clustering. Journal of Geophysical Research: Solid Earth 99, 2601–2618.

Van der Elst, N.J., 2021. b-positive: A robust estimator of aftershock magnitude distribution in incomplete catalogs. Journal of Geophysical Research: Solid Earth 126, e2020JB021027. URL: https://doi.org/10.1029/2020JB021027, doi:10.1029/2020JB021027.

Farrell, J., Husen, S., Smith, R.B., 2009. Earthquake swarm and b-value characterization of the yellowstone volcano-tectonic system. Journal of Volcanology and Geothermal Research 188, 260–276.

Fischer, T., Hainzl, S., Vlček, J., 2023. Fast migration episodes within earthquake swarms. Geophysical Journal International 235, 312–325.

Gomberg, J., Blanpied, M.L., Beeler, N., 1997. Transient triggering of near and distant earthquakes. Bulletin of the Seismological Society of America 87, 294–309.

Grassberger, P., Procaccia, I., 1983. Measuring the strangeness of strange attractors. Physica D: Nonlinear Phenomena 9, 189–208.

Gutenberg, B., Richter, C.F., 1944. Frequency of earthquakes in california. Bulletin of the Seismological Society of America 34, 185–188. URL: https://doi.org/10.1785/BSSA0340040185.

Helmstetter, A., Sornette, D., 2003. Importance of direct aftershocks in the etas model. Journal of Geophysical Research 108, 2047.

Hill, D.P., Pollitz, F., Newhall, C., 2015. Earthquake-volcano interactions. Physics Today 68, 38–45.

Hooft, E.E., Nomikou, P., Toomey, D.R., Lampridou, D., Getz, C., Christopoulou, M.E., VanderBeek, B.P., 2017. Backarc tectonism, volcanism, and mass wasting shape seafloor morphology in the santorini-christiana-amorgos region of the hellenic volcanic arc. Tectonophysics 712, 396–414.

Iaccarino, A.G., Picozzi, M., 2023. Detecting the preparatory phase of induced earthquakes at the geysers (california) using k-means clustering. Journal of Geophysical Research: Solid Earth 128, e2023JB026429.

Ide, K., Sornette, D., 2002. Oscillatory finite-time singularities in finance, population and rupture. Physica A: Statistical Mechanics and its Applications 307, 63–106.

Ihlen, E.A., 2012. Introduction to multifractal detrended fluctuation analysis in matlab. Frontiers in Physiology 3, 141. URL: https://doi.org/10.3389/fphys.2012.00141, doi:10.3389/fphys.2012.00141.

Kagan, Y., 1991. Fractal dimension of brittle fracture. Journal of Nonlinear Science 1, 1–16.

Kagan, Y.Y., 2002. Seismic moment distribution revisited. Geophysical Journal International 149, 731–754.

Kagan, Y.Y., 2007. Earthquake spatial distribution: The correlation dimension. Geophysical Journal International 168, 1175–1194.

Kanamori, H., Brodsky, E.E., 2004. The physics of earthquakes. Reports on Progress in Physics 67, 1429.

Kantelhardt, J.W., Zschiegner, S.A., Koscielny-Bunde, E., Havlin, S., Bunde, A., Stanley, H.E., 2002. Multifractal detrended fluctuation analysis of nonstationary time series. Physica A: Statistical Mechanics and its Applications 316, 87–114. URL: https://doi.org/10.1016/S0378-4371(02)01383-3, doi:10.1016/S0378-4371(02)01383-3.

Karakostas, V., Papadimitriou, E., Gospodinov, D., 2015. Magnitude scaling relations in the Corinth Rift and surrounding area (Greece). Bulletin of the Geological Society of Greece 43, 502–511.

Karavias, A., Anastasiou, D., Svigkas, N., Papanikolaou, X., De Astis, G., Atzori, S., Papoutsis, I., 2025. Santorini inflates again: Geodetic monitoring and modeling of the 2024-2025 volcanic unrest. Authorea Preprints .

Leclerc, F., Palagonia, S., Feuillet, N., Nomikou, P., Lampridou, D., Barrière, P., Dano, A., Ochoa, E., Gracias, N., Escartin, J., 2024. Large seafloor rupture caused by the 1956 amorgos tsunamigenic earthquake, greece. Communications Earth & Environment 5, 663.

Lemarchand, N., Grasso, J.R., 2007. Interactions between earthquakes and volcano activity. Geophysical Research Letters 34.

Lennartz, S., Livina, V., Bunde, A., Havlin, S., 2008. Long-term memory in earthquakes and the distribution of interoccurrence times. Europhysics Letters 81, 69001.

Lippiello, E., Petrillo, G., Godano, C., Papadimitriou, E., Karakostas, V., Anagnostou, V., 2025. 2025 santorini-amorgos crisis triggered by a transition from volcanic to regular tectonic activity. arXiv preprint arXiv:2504.21371 .

Metzler, R., Klafter, J., 2000. The random walk's guide to anomalous diffusion: a fractional dynamics approach. Physics reports 339, 1–77.

Michas, G., 2025. Spatiotemporal diffusion variability of injection-induced seismicity in enhanced geothermal systems. Pure and Applied Geophysics , 1–13.

Michas, G., Vallianatos, F., 2018. Modelling earthquake diffusion as a continuous-time random walk with fractional kinetics: the case of the 2001 agios ioannis earthquake swarm (corinth rift). Geophysical Journal International 215, 333–345.

Nandan, S., Sornette, D., 2022. Systematic comparison of space-time epidemic-type aftershock sequence models. Journal of Geophysical Research: Solid Earth 127, e2021JB023803. URL: https://doi.org/10.1029/2021JB023803, doi:10.1029/2021JB023803.

Newman, A.V., et al., 2012. Recent geodetic unrest at santorini caldera, greece. Geophysical Research Letters 39, L06309. doi:10.1029/2012GL051286.

Nishikawa, T., Ide, S., 2017. Detection of earthquake swarms at subduction zones globally: Insights into tectonic controls on swarm activity. Journal of Geophysical Research: Solid Earth 122, 5325–5343.

Nishimura, T., 2017. Triggering of volcanic eruptions by large earthquakes. Geophysical Research Letters 44, 7750–7756.

NOAIG, 2025. Hellenic unified seismic network: Earthquake catalog. URL: http://www.gein.noa.gr/en/. last accessed: 2025-05-01.

NOAIG - Institute of Geodynamics, National Observatory of Athens, 2025. Observations and preliminary results on the seismic sequence between santorini and amorgos. Euro-Mediterranean Seismological Centre Special Reports. URL: https://www.emsc-csem.org/Special_reports/?id=351.

Nomikou, P., Carey, S., Papanikolaou, D., Croff Bell, K., Sakellariou, D., Alexandri, M., Bejelou, K., 2012. Submarine volcanoes of the kolumbo volcanic zone ne of santorini caldera, greece. Global and Planetary Change 90–91, 135–151. doi:10.1016/j.gloplacha.2012.01.001.

Ogata, Y., 1988. Statistical models for earthquake occurrences. Journal of Geophysical Research 93, 6225–6240.

Ogata, Y., 1993. Detection of precursory relative quiescence before great earthquakes. Geophysical Journal International 113, 267–276.

Papazachos, B.C., Papazachou, C., 2003. The Earthquakes of Greece. Ziti Publications, Thessaloniki.

Passarelli, L., Rivalta, E., Jónsson, S., Hensch, M., Metzger, S., Jakobsdóttir, S.S., Maccaferri, F., Corbi, F., Dahm, T., 2018. Scaling and spatial complementarity of tectonic earthquake swarms. Earth and Planetary Science Letters 482, 62–70.

Roman, D.C., Cashman, K.V., 2006. The origin of volcano-tectonic earthquake swarms. Geology 34, 457–460.

Sawi, T.M., Manga, M., 2018. Revisiting short-term earthquake triggered volcanism. Bulletin of Volcanology 80, 1–9.

Schmid, F., Petersen, G., Hooft, E., Paulatto, M., Chrapkiewicz, K., Hensch, M., Dahm, T., 2022. Heralds of future volcanism: Swarms of microseismicity beneath the submarine kolumbo volcano indicate opening of near-vertical fractures exploited by ascending melts. Geochemistry, Geophysics, Geosystems 23, e2022GC010420. doi:10.1029/2022GC010420.

Schorlemmer, D., Wiemer, S., 2005. Earthquake size distribution: Power-law with exponent beta? Nature 434, 1086–1089.

Seropian, G., Kennedy, B.M., Walter, T.R., Ichihara, M., Jolly, A.D., 2021. A review framework of how earthquakes trigger volcanic eruptions. Nature Communications 12, 1004.

Shannon, C.E., 1948. A mathematical theory of communication. The Bell System Technical Journal 27, 379–423.

Shapiro, S.A., Rentsch, S., Rothert, E., 2005. Fluid-induced seismicity: Theory, modeling, and applications. Journal of engineering mechanics 131, 947–952.

Shelly, D.R., Moran, S.C., Thelen, W.A., 2013. Evidence for fluid-triggered slip in the 2009 mount rainier, washington earthquake swarm. Geophysical Research Letters 40, 1506–1512.

Shimizu, Y., Thurner, S., Ehrenberger, K., 2002. Multifractal spectra as a measure of complexity in human posture. Fractals 10, 103–116.

Sornette, D., 2006. Critical phenomena in natural sciences. Springer .

Sornette, D., Helmstetter, A., 2002. Occurrence of finite-time singularities in epidemic models¡? format?¿ of rupture, earthquakes, and starquakes. Physical Review Letters 89, 158501.

Taroni, M., Barani, S., Zaccagnino, D., Petrillo, G., Harris, P.A., 2024. A physics-informed stochastic model for long-term correlation of earthquakes .

Telesca, L., Lapenna, V., 2006. Measuring multifractality in seismic sequences. Tectonophysics 423, 115–123.

Telesca, L., Lapenna, V., Macchiato, M., 2004. Tsallis entropy in earthquake magnitude distributions: A case study in southern italy. Physica A: Statistical Mechanics and its Applications 332, 123–128.

Telesca, L., Lovallo, M., Molist, J.M., Moreno, C.L., Meléndez, R.A., 2015. Multifractal investigation of continuous seismic signal recorded at el hierro volcano (canary islands) during the 2011–2012 pre-and eruptive phases. Tectonophysics 642, 71–77.

Tsallis, C., 1988. Possible generalization of boltzmann-gibbs statistics. Journal of Statistical Physics 52, 479–487.

Uchide, T., Horikawa, H., Nakai, M., Matsushita, R., Shigematsu, N., Ando, R., Imanishi, K., 2016. The 2016 kumamoto–oita earthquake sequence: aftershock seismicity gap and dynamic triggering in volcanic areas. Earth, Planets and Space 68, 1–10.

Vallianatos, F., Michas, G., Papadakis, G., Tzanis, A., 2013. Evidence of non-extensivity in the seismicity observed during the 2011–2012 unrest at the santorini volcanic complex, greece. Natural Hazards and Earth System Sciences 13, 177–185.

Vallianatos, F., Papadakis, G., Michas, G., 2016. Generalized statistical mechanics approaches to earthquakes and tectonics. Proceedings of the Royal Society A: Mathematical, Physical and Engineering Sciences 472, 20160497.

Venegas-Aravena, P., Zaccagnino, D., 2025. Large earthquakes are more predictable than smaller ones. https://doi.org/10.31223/X5WH92 .

Yong-Ge, W., Zhong-Liang, W., Gong-Wei, Z., 2003. Small stress change triggering a big earthquake: A test of thecritical point hypothesis for earthquakes. Chinese physics letters 20, 1452.

Zaccagnino, D., Telesca, L., Doglioni, C., 2021. Different fault response to stress during the seismic cycle. Applied Sciences 11, 9596.

Zaccagnino, D., Telesca, L., Doglioni, C., 2022. Variable seismic responsiveness to stress perturbations along the shallow section of subduction zones: the role of different slip modes and implications for the stability of fault segments. Frontiers in Earth Science 10, 989697.

Zaccagnino, D., Telesca, L., Doglioni, C., 2023. Global versus local clustering of seismicity: Implications with earthquake prediction. Chaos, Solitons & Fractals 170, 113419.

Zaccagnino, D., Vallianatos, F., Michas, G., Telesca, L., Doglioni, C., 2024. Are foreshocks fore-shocks? Journal of Geophysical Research: Solid Earth 129, e2023JB027337.

Zahradnik, J., Sokos, E., Roumelioti, Z., Turhan, F., 2025. Positive isotropic components of the 2025 santorini-amorgos earthquakes .

Zechar, J.D., Zhuang, J., 2010. Risk and return: evaluating reverse tracing of precursors earthquake predictions. Geophysical Journal International 182, 1319–1326.

Author contributions

Conceptualization, D.Z.; methodology, D.Z. and L.T.; software, D.Z.; investigation, D.Z.; writing—original draft preparation, D.Z., G.M., L.T.; writing—review and editing, D.Z., L.T., G.M., F.V.; visualization, D.Z.;

supervision, F.V., L.T.; project administration, F.V. All authors have read and agreed to the published version of the manuscript.

Funding

This research received no external funding and supported by the National and Kapodistrian University of Athens.

Data availability

We analyzed data provided by the National Observatory of Athens and a relocated catalog of events for the spatial analysis of seismicity (NOAIG, 2025).
Data are available at http://www.gein.noa.gr/en/services/earthquake-catalogs/ and https://zenodo.org/records/15111649.
Fault lines plotted in Figure 1A are after Leclerc et al. (2024).

Conflicts of interest

The authors declare no conflict of interest.